

Hartree-Fock Theory of Hole Stripe States

Tae-Suk Kim^a, S.R. Eric Yang^b, and A.H. MacDonald^c

^a APCTP, 207-43 Cheongryangri-dong, Dongdaemun-gu, Seoul 130-012, Korea

^b Department of Physics, Korea University, Seoul, Korea

^c Department of Physics, Indiana University, Bloomington IN 47405

(November 23, 2018)

We report on Hartree-Fock theory results for stripe states of two-dimensional hole systems in quantum wells grown on GaAs (311)A substrates. We find that the stripe orientation energy has a rich dependence on hole density, and on in-plane field magnitude and orientation. Unlike the electron case, the orientation energy is non-zero for zero in-plane field, and the ground state orientation can be either parallel or perpendicular to a finite in-plane field. We predict an orientation reversal transition in in-plane fields applied along the $[\bar{2}33]$ direction.

73.40.Hm, 71.45.Lr, 73.20.Dx

Because of the macroscopic degeneracy of Landau levels, the physics of two-dimensional (2D) electron systems in strong external fields has been a fertile area for many-particle physics. Recently [1–4] the emergence of strongly anisotropic transport properties at low temperatures has been interpreted as evidence for the occurrence of the unidirectional charge-density-wave *stripe* states predicted by Hartree-Fock theory [5]. For conduction band Landau levels with orbital kinetic energy index $n > 2$ (filling factor $\nu > 4$), the putative stripe states occur instead of the strongly correlated fluid states responsible for the quantum Hall effect [6]. Although Hartree-Fock theory provides a clear motivation for stripe states [5], it cannot reliably predict the nature of the ground state because the energetic competition with fluid states is delicate [7]. Moreover, the transport properties of stripe states cannot be explained by Hartree-Fock theory, although they are consistent [8] with theories [9–11] of quantum-fluctuating stripes. For these reasons, the ability of Hartree-Fock theory to predict [12,13] the low resistance (parallel to stripe) direction in an in-plane magnetic field has played an essential role in establishing the stripe-state explanation of $N > 2$ anisotropic transport. A recent study [14] in which a reorientation transition in a wide quantum well sample is explained by Hartree-Fock theory is especially convincing in this respect.

The present work is motivated by the discovery [15] of anisotropic transport in 2D hole systems grown on GaAs (311)A substrates. In this case, anisotropic transport already occurs for $\nu \sim 5/2$, demonstrating that there are important differences between the electron and hole cases. The change is not unexpected, given the anisotropy of 2D hole band structure. We have generalized the Hartree-Fock theory of stripe states to the case of valence bands described by a the single-particle Luttinger Hamiltonian [16]. We find that strong orbital-quantum-number mixing leads to anisotropic effective electron-electron interactions and to a dependence of stripe energy on orientation even in the absence of an in-plane

magnetic field. This property favors the formation of a stripe state, consistent with experiment. The ground state orientation is not in general either parallel or perpendicular to the direction of a finite in-plane field when one is present.

To describe 2D hole gases grown along the [311] direction, it is convenient to choose a Cartesian coordinate system with [011], $[\bar{2}33]$ and [311] direction axes. The cubic coordinates in terms of which the Luttinger Hamiltonian is usually expressed are related to these coordinates by $k_a = \sum_i u_{ai} k_i$, $a = x, y, z$; $i = 1, 2, 3$ in both direct and reciprocal space. Here the u_{ai} are direction cosines. Each element of the Luttinger Hamiltonian is a quadratic form in the k_i 's. The two-dimensional hole gas is created by a GaAs (narrow gap) quantum well flanked by the AlGaAs (wide gap) barriers. Since the barrier lies in the range 100 – 400 meV and the energy scale of interest is ~ 10 meV, we take the barrier to be infinite. Single particle eigenspinors of the quantum well Luttinger Hamiltonian can be expanded in the form $\psi_{\vec{k}}(\vec{x}) = \sum_{i\alpha} c_{i\alpha}(\vec{k}) e^{i\vec{k}\cdot\vec{r}} \zeta_i(x_3) \chi_\alpha(\vec{x})$. Here the 2D wavevector $\vec{k} = (k_1, k_2)$ is a good quantum number, and $\zeta_i(x_3) \propto \sin(i\pi x_3/b)$ where b is the well width. Bloch functions $\chi_\alpha(\vec{x})$ are chosen such that when k_1 and k_2 are set to zero the Luttinger Hamiltonian takes a diagonalized form.

For the GaAs valence bands we have used the Luttinger model parameters $\gamma_1 = 6.85$, $\gamma_2 = 2.1$, and $\gamma_3 = 2.9$ and retained the first 20 subbands. A typical 2D band structure is illustrated in Fig. 1 by plotting constant energy contours for the lowest energy subband. Since our confinement potential has inversion symmetry, each energy band is doubly degenerate. For wider quantum wells, subband spacing is reduced and subband mixing is strengthened. Since cubic systems are *not* invariant under 90° rotations about the [311] direction, the 2D bands have lower than square symmetry. The constant energy contours are elongated in directions with larger effective mass. For the lowest subband, the Fermi sur-

face anisotropy is relatively weak near the zone center (Γ point), but gets stronger at larger $|\vec{k}|$. The effective mass is heavier (lighter) along k_2 than along k_1 direction close to (far away from) the zone center, and is smallest along the direction rotated from k_1 by 45° at larger $|\vec{k}|$. As we shall discuss later, the Fermi surface topology is manifested in anisotropic effective electron-electron interactions and ultimately in orientation-dependent stripe state energies.

When a magnetic field is applied, the subband spectrum consists of macroscopically degenerate Landau levels whose energies may be evaluated following familiar lines. In the Luttinger Hamiltonian, k_1 and k_2 are replaced by raising and lowering ladder operators, $k_1 = i(-a + a^\dagger)/\sqrt{2}\ell$ and $k_2 = (a + a^\dagger)/\sqrt{2}\ell$, with $\ell = (\hbar c/eB)^{1/2}$ and a Zeeman term is added to the Luttinger Hamiltonian [16], $H_Z = -\kappa\mu_B\vec{J} \cdot \vec{B}$. Here μ_B is the Bohr magneton and $\kappa = 1.2$ is an additional Luttinger model parameter. The envelope function eigen spinors can be expanded in the form $\psi_{nX}(\vec{x}) = \sum_{n_i\alpha} c_{n_i\alpha} \phi_{nX}(\vec{p}) \zeta_i(x_3) \chi_\alpha(\vec{x})$ where $\phi_{nX}(\vec{p})$ is one of the parabolic band Landau gauge wavefunction generated by the ladder operator algebra, and the Hamiltonian matrix is independent of the guiding center label X . The eigenstates of the Hamiltonian are strong mixture of Landau level n and subband i indices. In diagonalizing the finite-field Luttinger Hamiltonian, three subbands and 30 Landau levels were retained. This procedure is readily generalized to allow for a magnetic field component perpendicular to the growth direction, $\vec{B} = B(\hat{x}_3 + \tan\theta[\hat{x}_1 \cos\varphi + \hat{x}_2 \sin\varphi])$. In this case, $k_1 \rightarrow k_1 + \tan\theta \sin\varphi x_3/\ell^2$ and $k_2 \rightarrow k_2 - \tan\theta \cos\varphi x_3/\ell^2$.

Fig. 2 illustrates our results for the magnetic field dependence of the Landau level energies for a typical quantum well width and no in-plane field. The Landau levels show very strong nonlinear dispersion with magnetic field. The energy levels are unevenly spaced and the apparently crossed levels are split due to the lack of parity under the inversion symmetry operation. Both Landau-level and subband mixing are stronger at larger quantum well widths.

To model the stripe state seen in Ref. [15] at $\nu = 5/2$, we consider interacting electrons in the third level of Fig. 2 at $B \approx 2.5$ Tesla ($n_h = 1.5 \times 10^{11} \text{ cm}^{-2}$). The distorted semiclassical cyclotron orbit of a Fermi energy electron with this density is illustrated in Fig.1 for the case of $b = 250\text{\AA}$. Semiclassical orbit distortions translate quantum mechanically into mixing of parabolic band Landau levels. For interactions within a Landau level this mixing is described exactly [12] simply by replacing the Coulomb interaction by

$$V_{\text{eff}}(\vec{q}) = \frac{2\pi e^2}{q\epsilon(q)} \sum_{\{n_i\}} M_{n_1 n_4, n_2 n_3}(q) F_{n_1 n_4}(\vec{q}) F_{n_2 n_3}(-\vec{q}). \quad (1)$$

where $\epsilon(q)$ is the dielectric constant arising from polar-

ization of the lower filled Landau levels and

$$M_{n_1 n_4, n_2 n_3}(q) = \sum_{\alpha\beta} \sum_{\{i_i\}} c_{n_1 i_1 \alpha}^* c_{n_4 i_4 \alpha} c_{n_2 i_2 \beta}^* c_{n_3 i_3 \beta} W(i_1 i_4, i_2 i_3; q)$$

with

$$W(i_1 i_4, i_2 i_3; q) \equiv \int dz \int dz' e^{-q|z-z'|} \zeta_{i_1}^*(z) \zeta_{i_4}(z) \zeta_{i_2}^*(z') \zeta_{i_3}(z').$$

Note that $V_{\text{eff}}(\vec{q})$ is always repulsive. The parabolic-band plane-wave matrix elements, $F_{nn'}(\vec{q})$, play a crucial role since they are dependent on the 2D angular coordinate of \vec{q} , ϕ_q : $F_{n_1 n_4}(\vec{q}) F_{n_2 n_3}(-\vec{q}) \sim e^{i\pi(n_1+n_2-n_3-n_4)\phi_q}$. It is precisely this effect which gives rise to orientation dependence of the stripe state energy. In an electron gas, $n_1 = n_2 = n_3 = n_4 = N$ and the stripe state has no orientation dependence.

In the Hartree-Fock approximation, the energy per electron for the stripe state of a half-filled Landau level is [12]

$$E = \frac{1}{2\nu^*} \sum_{n=-\infty}^{\infty} \Delta_n^2 U\left(\frac{2\pi n}{a} \hat{e}\right), \quad (2)$$

where

$$\Delta_n = \nu^* \frac{\sin(n\nu^*\pi)}{n\nu^*\pi},$$

\hat{e} is the direction perpendicular to the stripes, ν^* the filling fraction at upper Landau level, and

$$U(\vec{q}) = \frac{V_{\text{eff}}(\vec{q})}{2\pi\ell^2} - \int \frac{d^2 p}{(2\pi)^2} V_{\text{eff}}(\vec{p}) e^{i(p_x q_y - p_y q_x)\ell^2}.$$

The evaluation of $U(\vec{q})$ is simplified by Fourier expanding the angle dependence of $V_{\text{eff}}(\vec{q})$ and taking advantage of inversion symmetry in the 2D plane. The isotropic Fourier component is most dominant near $q = 0$. Higher Fourier components vanish at $q = 0$, and oscillate between positive and negative values as a function of q . When summed, the net result is a strong suppression of $V_{\text{eff}}(\vec{q})$ at $q\ell > 1.5$, which helps to make $U(\vec{q})$ more negative (see Figure 3) and favors stripe states.

The results we obtain for the orientation dependence of the cohesive energy in a 250\AA quantum well are presented in Fig. 4. The ground state stripe orientation is tilted from the $[\bar{2}33]$ axis by $\phi_{\text{st}} \approx 23^\circ$. We studied the dependence of the ground state ϕ on well width, b , finding that for $b = 100\text{\AA}$ and less $\phi_{\text{st}} = 0^\circ$. On the other hand, for $b = 150\text{\AA}$ and $b = 200\text{\AA}$ [15], we find $\phi_{\text{st}} \approx 15^\circ$ and $\phi_{\text{st}} \approx 22^\circ$, respectively. The difference in cohesive energy per electron between $\phi = 0$ and ϕ_{st} , $|E_{\text{coh}}(0^\circ) - E_{\text{coh}}(\phi_{\text{st}})|$, is small: for $b = 150, 200, 250\text{\AA}$ it

is, respectively, 0.7, 2.8, 4.5% of the maximum difference $|E_{coh}(90^\circ) - E_{coh}(\phi_{st})|$. For larger values of $b = 300\text{\AA}$, 350\AA and 400\AA , we find $\phi_{st} \approx 45^\circ$. The ground state ϕ_{st} changes gradually from 0° to 45° with increasing quantum well width. Note that the dependence of the ground state stripe direction on well width tracks the well-width dependence of the Fermi surface topology.

We believe it is band anisotropy, and the orientation dependence of stripe-state energy it leads to, that is primarily responsible for the occurrence of hole stripe states at $\nu = 5/2$. In 2D electron gases, stripe states appear [4,7] at $\nu = 5/2$ only when anisotropy is imposed by adding an in-plane magnetic field. Comparing experiment [4] and in-plane field calculations [12], we find that conduction band stripe states appear at $\nu = 5/2$ when the intrinsic orientation energy per electron is $\sim 0.0002e^2/\epsilon_0\ell$, comparable to the valence band $\nu = 5/2$ orientation energy per hole at *perpendicular* fields illustrated in Fig. 4.

The valence band orientation energy is also sensitive to in-plane field as illustrated in Fig. 4 for $B \approx 2.5$ Tesla. For quantum wells of widths $b = 100 - 250\text{\AA}$, increasing in-plane field along the $[01\bar{1}]$ axis (Fig. 4(a): $\varphi = 0^\circ$) tends to orient the easy axis of striped CDW closer to $[\bar{2}33]$. On the other hand, when in-plane field is applied along $[\bar{2}33]$ axis (Fig. 4(b): $\varphi = 90^\circ$) we find that for a sufficiently large well widths and field tilt angles, the ground state orientation can change from near $[\bar{2}33]$ to $[01\bar{1}]$.

In comparing with experiment, it is necessary to use the appropriate sample width and 2D hole density and to account for the corrugations which occur [17] at GaAs/AlGaAs(311)A interfaces. For example, we have investigated the hole density dependence of the orientation energy and found that there is more anisotropy at higher hole densities as expected from Fig. 1. The consequences of corrugation for the stripe states are difficult to quantify, partly because the stripe state period does not match the period of corrugation potential. Nevertheless it is likely that this morphological feature is partly responsible [15] for the factor of ~ 2 mobility anisotropy at zero field and that it will tend to align the stripes. Taking account of the corrugations, our finding for the 200\AA quantum well case [15], is consistent with experimental finding that stripes are aligned along $[\bar{2}33]$. It is reasonable to conclude that the corrugation contribution to the orientation energy overcomes the small intrinsic value of $|E_{coh}(\phi = 0^\circ) - E_{coh}(\phi_{st})|$. Intrinsic orientation energies can, however, be altered by tilted fields. For fields along the $[01\bar{1}]$ direction, $E_{coh}(\phi = 90^\circ) - E_{coh}(\phi = 0^\circ)$ is increased and we would expect little experimental consequence. For fields along the $[\bar{2}33]$ direction, on the other hand, we predict a dramatic reversal of stripe orientations at tilt angle $\theta \sim 60^\circ$. At this angle, the intrinsic band-structure effects addressed here favor $[01\bar{1}]$ oriented stripes by $\sim 0.0008e^2/\epsilon_0\ell$ per electron. This number

should be compared with the $\sim 0.0001e^2/\epsilon_0\ell$ orientation energy produced [12] by a 25° field tilt in $n = 2$ conduction band Landau levels. In the $[100]$ growth conduction band case, stripes orient along $[110]$ directions for perpendicular fields, likely because of MBE growth stabilities analogous to the corrugations discussed above. The anisotropy energy produced by a $\sim 25^\circ$ field tilt, in the $n = 2$ conduction band case is sufficient to overcome this extrinsic anisotropy and reorient the stripes. Based on these comparisons, we conclude that tilted field effects can also overcome extrinsic anisotropy sources in the valence band case.

In summary, valence band stripe states have a finite orientation energy even without an in-plane field, favoring their occurrence at $\nu = 5/2$. For quantum well widths $b = 100 - 250\text{\AA}$, intrinsic band effects yield a ground state orientation close to $[\bar{2}33]$ and corrugation effects are likely sufficient to produce the $[\bar{2}33]$ orientation seen in experiment. We predict that for typical quantum well widths, an in-plane field applied along the $[\bar{2}33]$ direction will induce a stripe reorientation transition.

We are indebted to J.P. Eisenstein, T. Jungwirth, M. Shayegan, and R. Winkler for valuable discussions. This work was supported in part by the National Science Foundation under grant DMR-9714055, and in part by grant No.1999-2-112-001-5 from the interdisciplinary Research program of the KOSEF. We thank the Center for Theoretical Physics at Seoul National University for providing computing time.

-
- [1] M. P. Lilly, K.B. Cooper, J.P. Eisenstein, L.N. Pfeiffer, and K.W. West, Phys. Rev. Lett. **82**, 394 (1999).
 - [2] R.R. Du, D.C. Tsui, H.L. Stormer, L.N. Pfeiffer, K.W. Baldwin, and K.W. West, Solid State Commun. **109**, 389 (1999).
 - [3] W. Pan, R.R. Du, H.L. Stormer, D.C. Tsui, L.N. Pfeiffer, K.W. Baldwin, and K.W. West, Phys. Rev. Lett. **83**, 820 (1999).
 - [4] M.P. Lilly, K.B. Cooper, J.P. Eisenstein, L.N. Pfeiffer, and K.W. West, Phys. Rev. Lett. **83**, 824 (1999).
 - [5] A.A. Koulakov, M.M. Fogler, and B.I. Shklovskii, Phys. Rev. Lett. **76**, 499 (1996); Phys. Rev. B **54**, 1853 (1996); R. Moessner and J. T. Chalker, Phys. Rev. B **54**, 5006 (1996).
 - [6] See for example A.H. MacDonald in *Proceedings of the Les Houches Summer School on Mesoscopic Physics* (Elsevier, Amsterdam, 1995), edited by E. Akkermans, G. Montambaux, and J.-L. Pichard.
 - [7] E.H. Rezayi, F.D.M. Haldane, and Kun Yang, Phys. Rev. Lett. **83**, 1219 (1999).
 - [8] J.P. Eisenstein, M.P. Lilly, K.B. Cooper, L.N. Pfeiffer, and K.W. West, preprint [cond-mat/0003405], to appear in Physica E.

- [9] H.A. Fertig, Phys. Rev. Lett. **82**, 3693 (1999).
 [10] E. Fradkin and S.A. Kivelson, Phys. Rev. B **59**, 8065 (1999).
 [11] A.H. MacDonald, and Matthew P.A. Fisher, Phys. Rev. B **61**, 5724 (2000).
 [12] T. Jungwirth, A.H. MacDonald, L. Smrcka, and S.M. Girvin, Phys. Rev. B **60**, 15574 (1999).
 [13] T. Stanescu, I. Martin, and P. Phillips, Phys. Rev. Lett. **84**, 1288 (2000).
 [14] W. Pan, T. Jungwirth, H.L. Stormer, D.C. Tsui, A.H. MacDonald, S.M. Girvin, L. Smrcka, L.N. Pfeiffer, K.W. Baldwin, and K.W. West, preprint [cond-mat/0003483].
 [15] M. Shayegan, H.C. Manoharan, S.J. Papadakis, and E.P. De Poortere, Physica E **6**, 40 (2000). The sample studied in this experimental sample had a quantum well width $b = 200\text{\AA}$.
 [16] J.M. Luttinger, Phys. Rev. **102**, 1030 (1956).
 [17] R. Nötzel, N.N. Ledentsov, L. Däweritz, K. Ploog, and M. Hohenstein, Phys. Rev. B **45**, 3507 (1992).

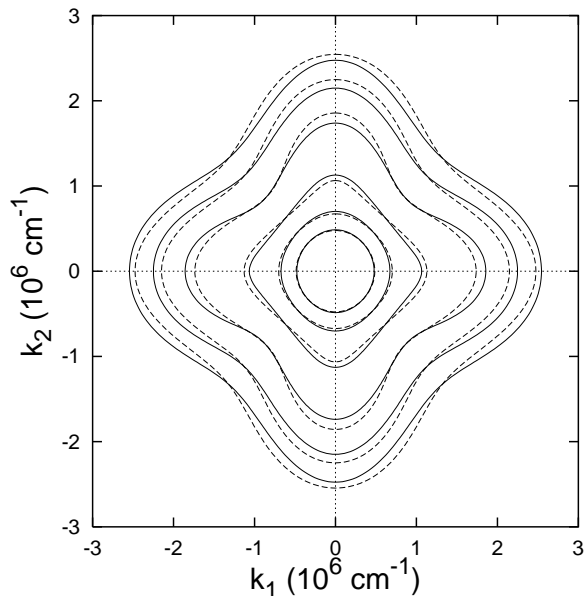


FIG. 1. Fermi surface topology for the well width 250\AA . The constant energy contour lines (solid lines) are drawn for the lowest subband. k_1 and k_2 correspond to $[01\bar{1}]$ and $[\bar{2}33]$ directions, respectively. (for illustration, rotated images of solid lines by 90° are displayed as dashed lines.) The energies for contours are 0.61, 1.1, 1.71, 2.31, 2.92, and 3.53 meV from inside to outside. Sample with $n_h = 1.5 \times 10^{11} \text{cm}^{-2}$ corresponds to the third contour ($E_F = 1.71 \text{meV}$).

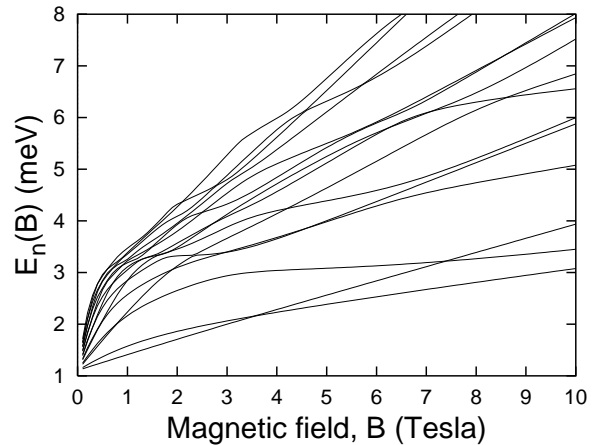


FIG. 2. Landau level dispersion with magnetic field. With the inclusion of the Zeeman term ($\kappa = 1.2$), the spin degeneracy is lifted.

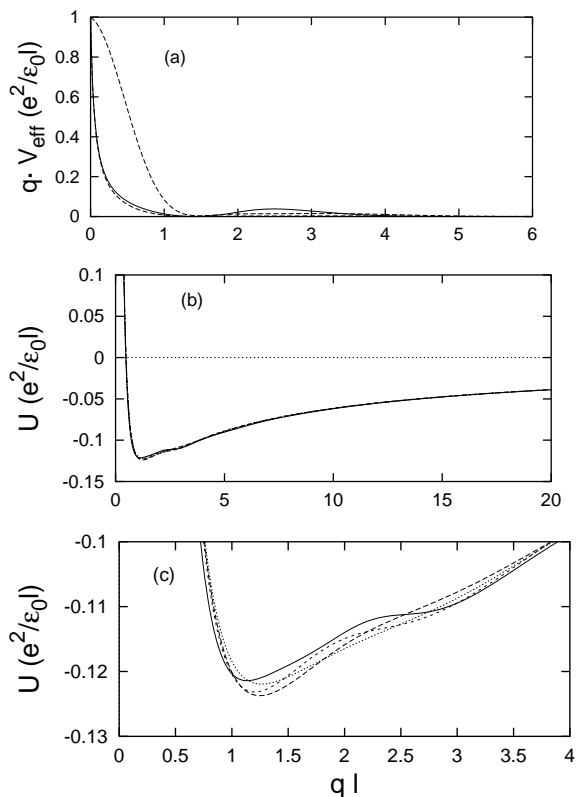


FIG. 3. Comparison of effective Coulomb potentials. (a) The Hartree potentials along $[01\bar{1}]$ are displayed for the quantum well of width 250\AA . Solid line corresponds to no-Landau-level-mixing case with screening. The upper (lower) dashed line represents unscreened (screened) Hartree potential for 2D holes at $\nu = 5/2$. (b) Hartree-Fock (HF) potentials. (c) Magnified view of HF potentials near the minimum where the angle dependence is significant. In (b) and (c), solid line: without Landau-level-mixing; long dashed line: along $[01\bar{1}]$; short dashed line: along 45° from x_1 axis; dotted line: along $[233]$.

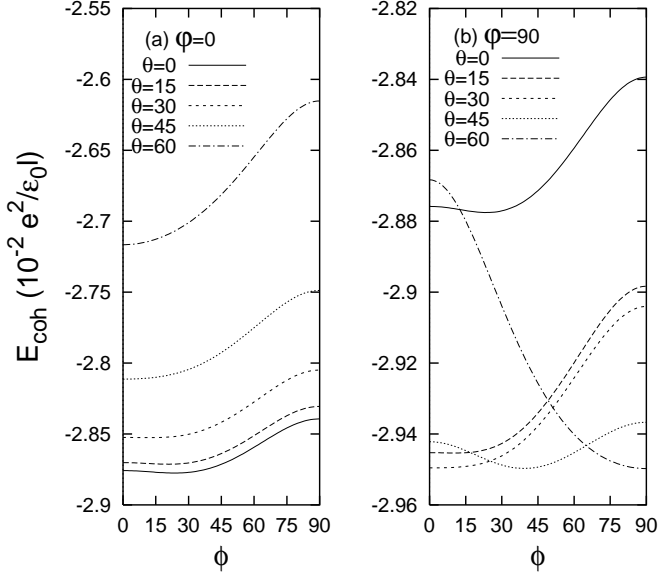


FIG. 4. The cohesive energy at $\nu = 5/2$ is drawn as a function of ϕ (the angle between $[233]$ and the easy axis of the striped CDW) with varying in-plane magnetic field for the confinement potential width 250\AA . Solid lines correspond to the case without in-plane fields. θ defines the direction of tilted magnetic fields from the $[311]$ axis. The in-plane fields are pointing along $[01\bar{1}]$ and $[233]$ in (a) and (b), respectively.